Ellipsometry Measurements on Refractive Index Profiles of Thin Films

JAU HWANG HO, CHUNG LEN LEE, AND TAN FU LEI

Abstract—**An ellipsometry technique to measure the arbitrary refractive index profile of composite thin films is presented. The refractive index profile is obtained through a successive partitioning and computation process on measured data points with the aid of a ϕ_0/T plot, which reduces errors. Analyses on the required number of data points in the partitioned sections, on the errors caused by the inappropriate partitioning, and on the cumulative errors have been performed. A $\Delta\phi_0/T$ plot is used to monitor the overall cumulative errors of the computation. Experimental examples by applying this technique to measure the refractive index profile of *O–N–O* and *O–N* composite thin films are included, and results are compared with those obtained by the Aüger electron spectroscopy (AES) technique. It is shown that this method is sensitive enough to determine the refractive index profile to a resolution of 20 Å.**

I. Introduction

In present VLSI MOS devices, compound thin films such as nitridized-SiO_2 or $SiO_2/Si_3N_4/SiO_2$ dielectrics have been used as the gate materials [1]–[5]. Much research work has been carried on the preparation, characterization and analysis of these dielectric films [6]–[10]. One of the techniques to characterize thin films is ellipsometry which can determine the refractive index and the thickness of films. It is very simple to apply, and its sensitivity and precision are rather high [11]–[17]. To measure the refractive index profile of thin films by using ellipsometry, a chemical thinning process is usually employed. The sample is repeatedly measured with ellipsometry and then chemically thinned to obtain successively changing ellipsometric data (Δ, φ). These are then substituted into the set of ellipsometry equations

$$f(\Delta, \varphi, \phi_0, N_s, K_s, N_2, T_2, N_1, N_0, \lambda) = T_1 \quad (1)$$

$$g(\Delta, \varphi, \phi_0, N_s, K_s, N_2, T_2, N_1, N_0, \lambda) = 0 \quad (2)$$

to solve for N_1, the refractive index, and T_1, the thickness of the etched layer of the sample, assuming a double-layer model [18]. In (1) and (2), ϕ_0 and λ are the incident angle and the wavelength of the monochromatic light, respectively, N_s-iK_s, N_2, N_1 and N_0 are the refractive indexes of the substrate, the bottom surface layer, the top surface layer and the ambient medium, respectively.

Manuscript received April 3, 1989; revised March 24, 1990. This work was supported by National Science Council, R.O.C. under Contract NSC 79-0404-E009-08.

The authors are with the Institute of Electronics, National Chiao Tung University, Hsinchu, Taiwan, R.O.C.

IEEE Log Number 9036460.

Errors in this procedure are usually introduced during computation due to the inherent measurement errors in parameters such as Δ, φ, and ϕ_0. As a result, the N–T profile obtained is not accurate. In 1983, Charmet *et al.* [19] derived ellipsometric formulas for an arbitrary refractive index profile by using Fourier transformations, and multiple-angle ellipsometry was used to determine the refractive index profile. However, the accuracy issue was not addressed and no experimental data were taken. We have studied the effect on accuracy caused by errors in the ellipsometric parameters and have proposed a scheme to improve the accuracy [20], [21]. This is based on a double-layer model to compute the index of refraction and the thickness of the surface thin film.

In this paper, the scheme is modified and applied to measure compound thin films of arbitrary refractive index profiles. The errors are reduced by taking a large number of data points on the sample. The required number of data points to achieve the error bound goal is also investigated. The refractive index profile is obtained through a procedure of data point partitioning. The error introduced during computation of the refractive index profile due to inappropriate partitioning of data points is also studied. Experimental examples of applying this method are included and the results obtained are compared with those obtained by the AES technique. The new method is especially sensitive in determining the index of refraction of the surface layer (within 20 Å) of thin films.

II. Description of the Technique

It has been shown [20], [21] that, in an ellipsometry measurement, two types of errors, namely the systematic errors and random errors, affect the accuracy of measurement. In order to minimize the effect of these errors, more than one measurement data are required for computing the refractive index. In particular, to minimize the effect of random errors, which are due to the instrumental resolution limitation in Δ and φ readings of the ellipsometer, it is desired to have as many as possible measurement data on one measured thickness. An averaging technique by plotting a ϕ_0/T_1 plot of these data could remove the random errors. In order to acquire a large number of measurement data, a sample area larger than 2 cm^2 is required. The thin film is uniformly deposited (or grown) on the surface of the sample. The sample is then gradually immersed into an etching solution (e.g., buffered HF so-

0018-9456/90/0800-0642$01.00 © 1990 IEEE

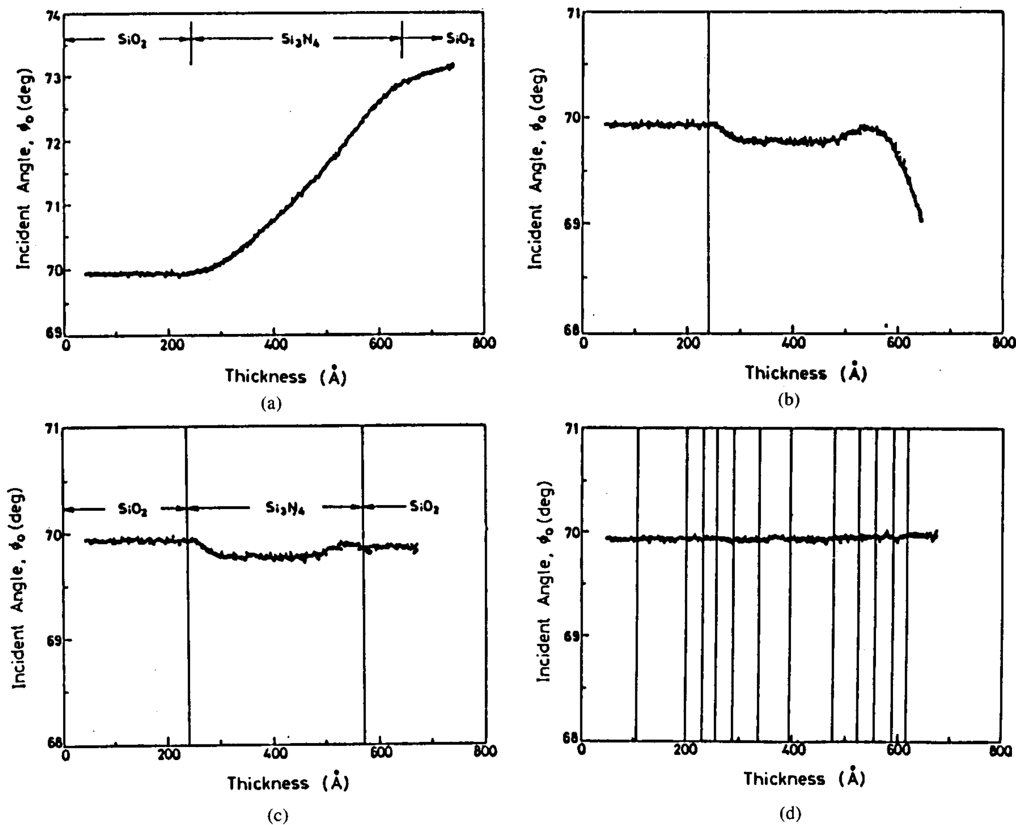

Fig. 1. (a) The ϕ_0/T plot of (Δ, φ) data measured on a composite $SiO_2/Si_3N_4/SiO_2$ film. For all three layers, the estimated N_1 is 1.463. (b) The ϕ_0/T plot for the sample of (a), but for the SiO_2 layer, the estimated refractive index is 1.463, and for the Si_3N_4 and the outer SiO_2 layers, the estimated refractive index is 1.946. (c) The same ϕ_0/T plot as in (b), but for the outer SiO_2 layer, the estimated refractive index is 1.491. (d) The same ϕ_0/T plot as in (c), but with thirteen partitioned sections.

lution for a SiO_2 film) to obtain a bevelled surface on the film. As the light beam of the ellipsometer is scanned across the bevelled surface of the thin film, the (Δ, φ) data corresponding to various thicknesses of the film are thus obtained. This procedure can be repeated (usually 3 times for a 100 Å film) to increase the number of data points. In this way, it is easy to acquire as many as 200 data points for a 100 Å thin film.

After the ellipsometric measurement, the obtained (Δ, φ) data are fed into (1) and (2) to compute for the incident angle, ϕ_0, and the film thickness, T_1, according to the technique in [21]. A ϕ_0/T_1 graph can be plotted. The ϕ_0/T_1 plot is computed by estimating a value for the index of refraction N_1 of the measured film. If the estimated N_1 value is correct, the plotted ϕ_0/T_1 diagram will be a horizontal line. It is obvious that, for a nonhomogeneous film, this ϕ_0/T_1 diagram will not be a horizontal line. However, a step-by-step estimating procedure can eventually achieve a horizontal ϕ_0/T_1 plot. This is demonstrated by using the following experimental example.

Fig. 1(a) is a ϕ_0/T_1 plot for a sample which has a compound Si(sub.)$/SiO_2/Si_3N_4/SiO_2$ structure. The sample was prepared by first growing an oxide(SiO_2) of approximately 250 Å, and then depositing a chemical vapor deposition (CVD) Si_3N_4 of approximately 400 Å on a Si substrate. The sample was then reoxidized at 1000°C for 40 min in a H_2O ambient to obtain an oxidized nitride layer. The ϕ_0/T_1 plot of Fig. 1(a) was obtained by estimating an $N_1 = 1.463$ which is the refractive index of the inner SiO_2 layer. It is seen that this estimated ϕ_0/T_1 plot could be roughly divided into three parts, i.e., the inner SiO_2 layer, for which the ϕ_0/T_1 plot shows a horizontal line, the Si_3N_4 layer and the outer oxidized nitride layer, which each have tilted ϕ_0/T curves. The Si_3N_4 layer and the oxidized nitride layer have tilted ϕ_0/T curves because their refractive indexes deviate from the estimated N_1 value of 1.463. It can also be observed that, there is a boundary between the Si_3N_4 layer and the oxidized nitride layer since the slopes of these two regions are different. From this ϕ_0/T plot, it can be seen that, the estimating

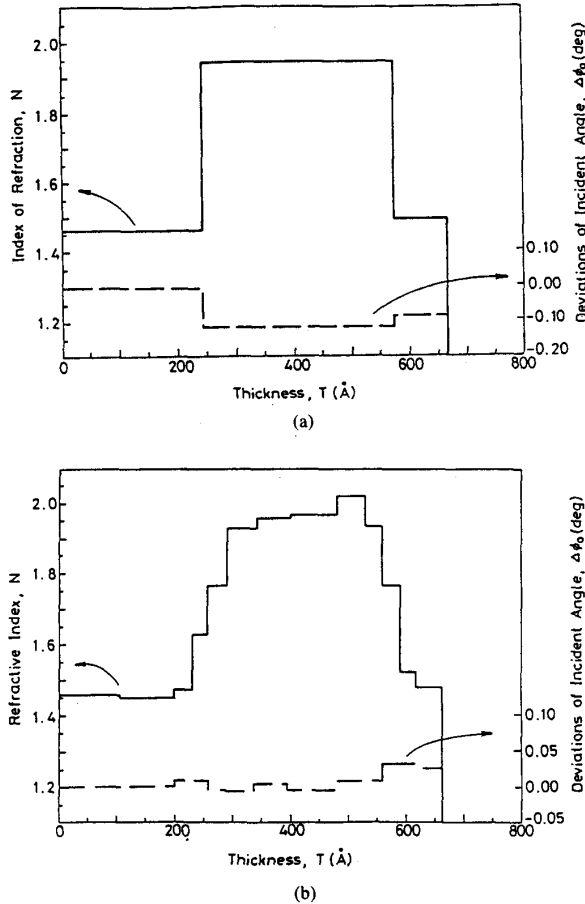

Fig. 2. (a) The obtained refractive index profile and the computed deviations of incident angle, $\Delta\phi_0$ of the $SiO_2/Si_3N_4/SiO_2$ film whose corresponding $\Delta\phi_0/T$ plot is shown in Fig. 1(c). (b) The computed refractive index profile as in (a), but with thirteen partitioned sections. The corresponding ϕ_0/T plot is shown in Fig. 1(d).

on N_1 can be divided into three steps. First, the refractive index of the inner SiO_2 is estimated and the ϕ_0/T plot is computed. From the obtained ϕ_0/T plot, the boundary between the SiO_2 and the Si_3N_4 layers can be identified. In Fig. 1(a), it is T_1 = 240 Å for N_1 = 1.463. These obtained N_1 and T_1 values can be used to compute the next estimated N value and the ϕ_0/T plot for the outer successive layers based on the double-layer model [21]. Fig. 1(b) is the obtained ϕ_0/T plot for this step of computation by estimating the refractive index for the Si_3N_4 layer to be 1.946. The boundary between this Si_3N_4 layer and the oxidized nitride layer is at T = 572 Å, where the slope of the ϕ_0/T plot shows tilting downward. Finally, the same computation process is applied to the third layer again by estimating N = 1.491 and the ϕ_0/T curve is plotted in Fig. 1(c). It is seen that the ϕ_0/T plot shows a nearly horizontal curve. The computed refractive index profile is shown in Fig. 2(a).

In the preceding computation process, the computation can be divided into more steps. Fig. 1(d) is the ϕ_0/T plot on the same set of measured (Δ, φ) data as that for Fig. 1(c) but with thirteen computation steps. A much more linear ϕ_0/T plot is obtained. The corresponding computed detail refractive index profile is shown in Fig. 2(b). This shows that the boundaries between the SiO_2 layer and the CVD Si_3N_4 layer, and between the CVD Si_3N_4 layer and the outer oxidized nitride layer are rather vague.

III. Discussion on Errors

In this technique, errors may be introduced due to inappropriate partitioning of measurement data. These errors are discussed in this section.

A. Random Errors Versus the Number of Measurement Data Points

In the previous section, it has been shown that more partitionings of the measured data can enhance the resolution of the refractive index profile and a truer refractive index profile can be obtained. However, the number of partitionings can not be arbitrarily increased. This number is limited by the required number of data points within one partitioned section for the guaranteed error reduction on random errors in (Δ, φ) readings. In this section we study how many data points are required to achieve the required accuracy.

The study is based on a statistical treatment to estimate the random errors on the refractive index. The physical model used is the double-layer model [21]. In the model, T_1 is the partitioned section whose refractive index and thickness are to be computed and T_2 is the effective lumped layer whose effective refractive index and thickness have been determined. For the partitioned section T_1, there are m data points which are measured for thin films of different thickness within the T_1 range.

For the type of the ellipsometer used in this study, the instrumental scale resolution for Δ and φ are $1°/12$ and $1°/24$, respectively. Hence, during one reading, (Δ, φ) could be one of the following nine combinations: ($\Delta + 1°/12$, $\varphi + 1°/24$), ($\Delta + 1°/12$, φ), ($\Delta + 1°/12$, $\varphi - 1°/24$), (Δ, $\varphi + 1°/24$), (Δ, φ), (Δ, $\varphi - 1°/24$), ($\Delta - 1°/12$, $\varphi + 1°/24$), ($\Delta - 1°/12$, φ) and ($\Delta - 1°/12$, $\varphi - 1°/24$). For m measurements on different film thickness, the total number of possible combinations of (Δ, φ) readings is 9^m. The average error on this refractive index for the m data points can be defined as

$$\delta N_{avg} = \left[\frac{\sum_{i=1}^{9^m} \delta N_{(i)}^2}{9^m} \right]^{1/2} \tag{3}$$

where $\delta N_{(i)}$ is the ith error corresponding to the ith possible (Δ, φ) values. This δN_{avg} can be computed in the following way.

If, in this partitioned section, these m data are distributed uniformly throughout the film thickness, T_1, δN_{avg} in

(3) can be evaluated to be [22]

$$\delta N_{avg} = \left\{ \frac{2m}{9} (\delta n_{1,1} \delta n_{m,1} + \delta n_{1,2} \delta n_{m,2} + \delta n_{1,3} \delta n_{m,3} + \delta n_{1,4} \delta n_{m,4}) + \frac{m(2m-1)}{27(m-1)} [(\delta n_{1,1} - \delta n_{m,1})^2 + (\delta n_{1,2} - \delta n_{m,2})^2 + (\delta n_{1,3} - \delta n_{m,3})^2 + (\delta n_{1,4} - \delta n_{m,4})^2] \right\}^{1/2}. \quad (4)$$

In (4), the denotations $\delta n_{i,1}$, $\delta n_{i,2}$, $\delta n_{i,3}$, $\cdots$, and $\delta n_{i,9}$ represent the errors of refractive index for errors occurring only in the ith data due to the nine possible data caused by the effects of the resolution. For example, $\delta n_{m,4}$ represents the refractive index error δn which occurs when the φ value has a $1°/24$ deviation in the mth data point. This simple formula can be used to estimate the errors caused by inadequacy of data points within T_1.

Equation (4) is computed and plotted in Fig. 3 in terms of the density of data for various T_1 thicknesses assuming $N_2 = 1.46$, $T_2 = 400$ Å, and $N_1 = 2.00$. (These values of data give the worst case estimation). It is seen that δN_{avg} decreases if the density of data increases. For $T_1 = 20$ Å, the density of data needed to obtain an error less than 0.03 for its refractive index of 2.00 (this corresponds to a 1.5% error) is approximately 2 data points/Å. In practice, this is the data density which can be achieved without too much difficulty. In the figure, in addition, the δN_{avg} is smaller for thicker T_1. For example, the errors for $T_1 = 40$ Å are almost two times lower than those for $T_1 = 20$ Å. Hence, if the density of data is fixed and high accuracy is demanded, a thicker subsection can be chosen. The ultimate data density which can be obtained for the type of ellipsometer which has $1°/12$ and $1°/24$ instrumental resolutions for Δ and φ readings, respectively, is approximately 19 data points/Å.

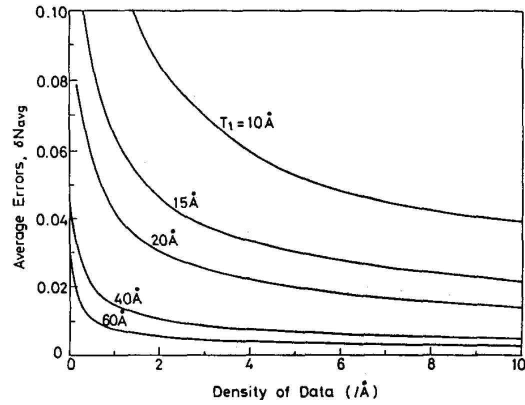

Fig. 3. Plots of the estimated averaged errors in terms of the density of measurement data for various T_1 values assuming $N_2 = 1.46$, $T_2 = 400$ Å, and $N_1 = 2.00$.

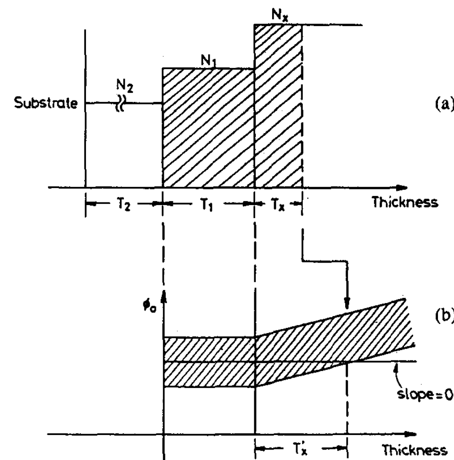

Fig. 4. (a) A model for a sample of three layers with refractive indexes N_x, N_1, and N_2, respectively, and thicknesses T_x, T_1, and T_2, respectively. (b) The computed ϕ_0/T graph for a estimated N_1 with the (Δ, φ) data of the intermediate and outer layers in (a). The shaded region is due to the spreading of the data. The T_x', which corresponds to the thickness T_x in (a), is determined by the intersection of the horizontal fitted line with the band edge of the tilted band.

B. Errors Due to the Inaccurate Partitioning

To compute the refractive index profile, it is very possible that the partitioning of data points is not at the true boundaries of the composite thin film. This inaccurate partitioning also leads to errors discussed in the following.

Fig. 4(a) shows a composite thin film with 3 layers of different refractive indexes. It is assumed that N_2 and T_2 of the inner layer are known, and the ϕ_0/T plot of this layer is the horizontal band shown in Fig. 4(b). For the intermediate layer, the N_1 and T_1 are to be computed by partitioning the (Δ, φ) data. Suppose that this partitioning is not at the boundary of N_1 and N_x, which is the outer layer that has another refractive index value, and instead, it is at some position T_x within the outer layer. The (Δ, φ) data which belong to the N_x layer are grouped into those of the N_1 layer (the shaded regions of Fig. 4(a)). The computed values for N_1 and T_1 will then deviate from the true values of N_1 and T_1.

Fig. 5 shows the computed errors caused by this bad partitioning for $N_2 = 1.46$, $T_2 = 300$ Å, $N_1 = 1.60$, $T_1 = 50$ Å in terms of T_x for various N_x. It is seen that the error is proportional to the difference between N_1 and N_x. For all N_x values, the error increases rapidly with T_x until $T_x = 10$ Å and then decreases. For $T_x = 50$ Å, the error becomes insignificant (< 0.003).

In practice, T_x can be kept to within 10 Å by manually selecting the boundary of T_1 from the ϕ_0/T_1 plot. The error introduced is negligible. For example, in Fig. 4(b), the fitted line of the zero slope for the first section, T_1 intersects the band edge of the tilted band at T_x'. If $N_1 = 1.60$, and $T_1 = 50$ Å, the error in δN_1 caused by includ-

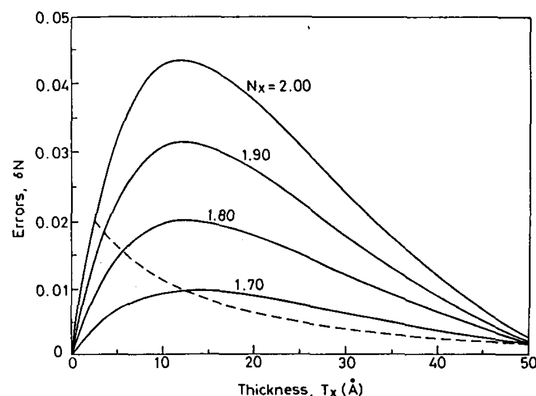

Fig. 5. The plot of errors produced in the computed refractive index in terms of the partitioning T_x error for various N_x values. For this computation, $N_2 = 1.46$, $T_2 = 300$ Å, $N_1 = 1.60$, and $T_1 = 50$ Å. The dotted line is the error in the refractive index caused by including the (Δ, φ) data in T_x' to compute N_1 for various N_x values.

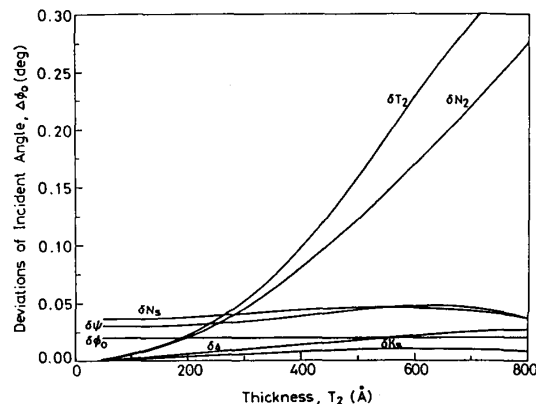

Fig. 6. The plot of the deviations in incident angle caused by the errors in various parameters: Δ, φ, ϕ_0, N_s, K_s, N_2, and T_2, in terms of the thickness T_2.

ing the (Δ, φ) data in T_x' to compute for N_1 is shown in Fig. 5 in the dotted line for various N_x values. The error is smaller than 0.02. In this example, for $N_x = 1.70$, T_x is approximately 10 Å. This means that, for a refractive index profile, if there is a 0.10 ($N_x = N_1 = 0.10$) refractive index difference between two adjacent sections within 10 Å, this method is able to differentiate the refractive indices of these two sections. Hence, this method can offer a resolution of 20 Å in measuring the refractive index of the surface of a thin film. In Section IV on experiments, an example is to be shown to demonstrate this capability.

C. Cumulative Errors and Error Monitoring

In this section, a method is presented to monitor the cumulative errors for a computed refractive index profile after having gone through the above successive partitioning and computing process.

It has been mentioned [20] that the variations in Δ, φ, N_s, K_s, etc., can be lumped into an effective deviation in ϕ_0, i.e., $\Delta\phi_0$, and the errors introduced due to the above parameters are equivalent to the error introduced in $\Delta\phi_0$. The effective $\Delta\phi_0$ caused by each deviation in Δ, φ, N_s, K_s, N_2, and T_2 for a double-layer model are computed, respectively. They are shown in Fig. 6 in terms of the film thickness of T_2. To compute the curves in Fig. 6, N_2, N_1 and T_1 are chosen to be 1.46, 2.00, and 20 Å, respectively, and the deviations: $\delta\Delta$, $\delta\varphi$, $\delta\phi_0$, δN_s, δK_s, δN_2, and δT_2 are assumed to be $1°/12$, $1°/24$, 0.02°, 0.008, 0.008, 0.02, and 2%, respectively. The true incident angle, ϕ_0 is 70.00°. It is seen that, among the parameters, N_2 and T_2 cause the most deviation in ϕ_0, especially when $T_2 > 300$ Å. $\Delta\phi_0$ caused by other parameters are generally smaller than 0.05° for all T_2 regions < 800 Å. N_2 and T_2, in this method, are the computed effective refractive index and thickness of the inner sections during the previous computation. It is thus concluded that the errors in the previously computed N_2 and T_2 have the largest effect on the computed incident angle for the next partitioned section. Hence, it is possible to gain information on the accuracy of the computation by observing the $\Delta\phi_0$ caused by the previously computed N_2 and T_2.

In the ϕ_0/T graph, for each partitioned section, a value for ϕ_0 is obtained for the corresponding computed N_1 and T_1. This value of ϕ_0 generally deviates from the exact value of ϕ_0, which is 70.00°, due to the errors in the previously computed N_2 and T_2. The difference between these two values is $\Delta\phi_0$ for this computed section. This $\Delta\phi_0$ can be plotted in terms of T along with the ϕ_0/T graph. By observing the $\Delta\phi_0/T$ plot, we can tell the accuracy of the computation.

Fig. 2(b) is the example of the refractive index profile of the Si(sub.)/SiO_2/Si_3N_4/SiO_2 compound thin film, where the corresponding $\Delta\phi_0/T$ plot is also shown as the dotted line. For this computed profile, it is seen that $\Delta\phi_0$ never exceeds 0.04°. This means that the errors in the final computed refractive index profile never exceeds 0.005 (from Fig. 6). In Fig. 2(a), the refractive index profile and its corresponding $\Delta\phi_0/T$ plot of the same sample are also included. These are computed based on the same (Δ, φ) data but with three partitionings. It is seen that this $\Delta\phi_0/T$ plot varies in much larger magnitude for each section. The average $\Delta\phi_0$ is $-0.1°$, which corresponds to an 0.015 average error in the final refractive index profile computation. In practice, $\Delta\phi_0$ can be chosen to be within $\pm 0.1°$. The error for the computed refractive index profile can be guaranteed to be less than 0.02.

IV. Experimental Results

This technique has been used to study the refractive index profile of nitridized silicon dioxides and poly-silicon dioxides [23]. In this section, two experimental examples of applying this technique are demonstrated. They are: (1) the *O–N–O* structure of Fig. 1, and (2) a nitridized silicon dioxide. For both cases, the composition depth profiles obtained separately by the AES technique are included for comparison.

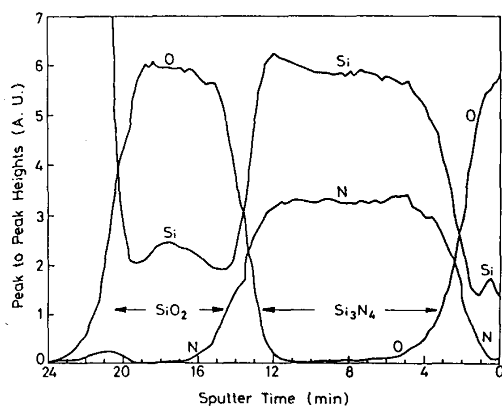

Fig. 7. The AES depth profile for the $SiO_2/Si_3N_4/SiO_2$ composite film, whose refractive index profile is shown in Fig. 2(b).

A. The O-N-O Structure

The detailed refractive index profile and the ϕ_0/T have been shown in Fig. 2(b). The corresponding AES composition profiles are shown in Fig. 7. The peak-to-peak heights of Si(LVV), N(KLL) and O(KLL) transitions are shown in terms of the sputter time. It is seen that these profiles have a good similarity with that of Fig. 2(b). However, Fig. 2(b) gives a much clearer depiction of the profile.

B. The Nitridized SiO_2 Structure

It had been reported that the thermal nitridation of silicon dioxide results in a compositional profile that varies with the depth [1]-[5]. Here, the refractive index profile of nitridized silicon dioxide films are measured by this ellipsometric method.

Fig. 8(a) shows the measured refractive index profile of a SiO_2 film nitridized at 1100°C for 5 h. It is seen that the refractive index was nearly constant throughout the film except that near the surface a thin layer of a 21 Å thickness with $N = 1.82$ existed. In the figure, the $\Delta\phi_0/T$ plot is also included. The cumulative error is seen to be very small. Fig. 8(b) is the ϕ_0/T plot for the profile of Fig. 8(a) near the surface region after the bulk refractive index had been computed. From this figure, the refractive index at this region is observed to be significantly higher than that of the bulk region. Hence, from this example, it is seen that this technique can detect the refractive index variation of a layer even as thin as 20 Å. The AES data for this sample are shown in Fig. 8(c). It is observed that there were nitrogen and silicon pile-ups near the surface, which might make the refractive index higher. Comparing the AES profiles of Fig. 8(c) with the refractive index profile of Fig. 8(a), both figures show the same trend. However, the refractive index profile obtained by this method reveals a much clearer picture on this nitridized SiO_2 film.

Fig. 9 shows another measured refractive index profile by this method for a SiO_2 sample which was nitridized in pure ammonia gas at 1100°C for 3 min. It is seen that for this sample, a thin (approximately 20 Å) nitrogen-rich layer of a refractive index of 1.70 also existed. There was also a nitrogen-rich interface of silicon substrate and the nitridized film. This phenomenon had also been observed

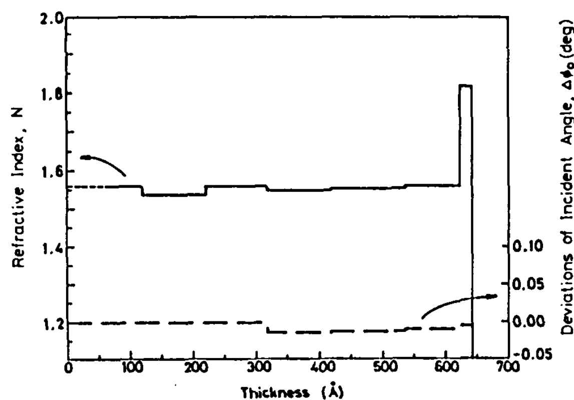

(a)

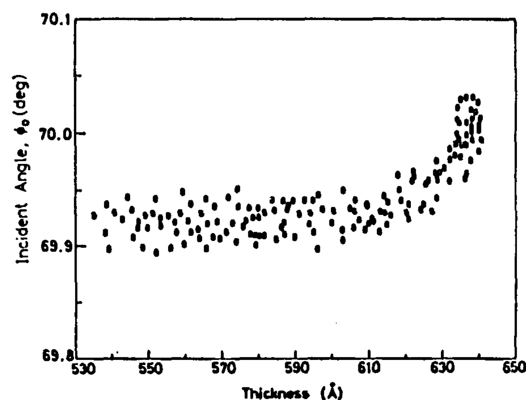

(b)

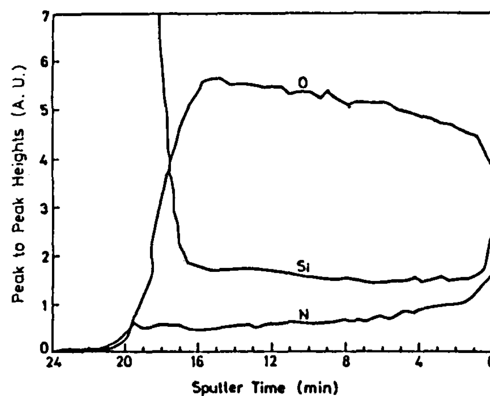

(c)

Fig. 8. (a) The computed refractive index profile (the solid line) and the incident angles (the dotted line) for the SiO_2 films after the 1100°C and 5-h NH_3-nitridation process. (b) The ϕ_0/T_1 plot for measurement data near the surface of the nitridized-SiO_2 film. The estimated refractive index is 1.55 during the computation. (c) The AES depth profile for the nitridized-SiO_2 film of (a).

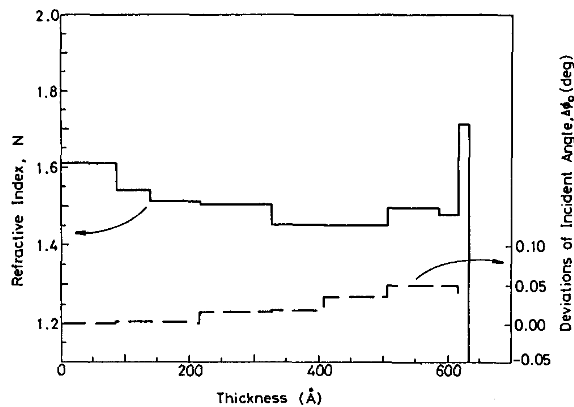

Fig. 9. The computed refractive index profile (the solid line) and the incident angles (the dotted line) for the SiO_2 films after the 1100°C and 3-min NH_3-nitridation process.

in [1]–[5]. In the figure, the $\Delta\phi_0/T$ plot is also included and the maximum deviation in $\Delta\phi_0$ was within 0.05° which was very small.

V. Conclusions

An ellipsometry measurement technique to measure the refractive index profile of composite thin films has been proposed and demonstrated. This technique employs the error reduction scheme of [20], [21] to reduce the systematic and random errors. The profile is obtained through a procedure of partitioning the (Δ, φ) data. The errors introduced due to inappropriate partitionings are discussed and studied. It is found that for a partitioned section of a 20 Å thickness, 40 data points are enough to obtain an error less than 0.03 for a refractive index of 2.0. In practice, this is a datum density easily achieved by scanning the laser beam of the ellipsometer over the etched bevelled surface of the sample for three times. The errors caused by bad partitionings are usually negligible. For two adjacent sections with 0.10 refractive index difference, the thickness differentiable from the ϕ_0/T plot can be as thin as 10 Å. From experiments, this method has been shown to be able to offer a resolution of 20 Å in measuring the refractive index of the surface of a thin film. A $\Delta\phi_0/T$ plot has also been proposed to monitor the cumulative errors through the partitioning and computation process. This helps to minimizing the errors caused by inaccurate partitioning.

In this paper, all the computations were done on SiO_2 or Si_3N_4 films in the thickness range of 100–800 Å. However, this method can be applied to other composite films with other thickness ranges.

Acknowledgment

The authors wish to thank T. S. Chao for his help in preparing the manuscript.

References

[1] S. S. Wong, C. G. Sodini, T. W. Ekstedt, H. R. Grinolds, K. H. Jackson, S. H. Kwan and W. G. Oldham, "Low pressure nitrided-oxide as a thin gate dielectric for MOSFET's," *J. Electrochem. Soc.*, vol. 130, pp. 1139–1144, 1983.

[2] M. M. Moslehi and K. C. Saraswat, "Thermal nitridation of Si and SiO_2 for VLSI," *IEEE Trans. Electron. Devices*, vol. ED-32, pp. 106–123, 1985.

[3] M. M. Moslehi, C. J. Han, K. C. Saraswat, C. R. Helms, and S. Shatas, "Compositional studies of thermally nitrided silicon dioxide (nitroxide)," *J. Electrochem. Soc.*, vol. 132, pp. 2189–2197, 1985.

[4] T. Watanabe, A. Menjoh, M. Ishikawa, and J. Kumagai, "Stacked $SiO_2/Si_3N_4/SiO_2$ dielectric layer for reliable memory capacitor," in *IEDM Tech. Dig.*, pp. 173–176, 1984.

[5] S. K. Lee, Y. H. Ku, D. K. Shih, D. L. Kwong, B. Y. Nguyen, and K. W. Teng, in *IEDN Tech. Dig.*, p. 93, 1987.

[6] S. P. Murarka, C. C. Chang and A. C. Adams, "Thermal nitridation of silicon in ammonia gas: Composition and oxidation resistance of the resulting films," *J. Electrochem. Soc.*, vol. 126, pp. 996–1003, 1979.

[7] J. Amano and T. Ekstedt, "Characterization of thermally nitrided silicon dioxide," *Appl. Phys. Lett.*, vol. 41, no. 9, pp. 816–818, Nov. 1982.

[8] F. H. P. M. Habraken, E. J. Evers, and A. E. T. Kuiper, "Hydrogen content of thermally nitrided thin silicon dioxide films," *Appl. Phys. Lett.*, vol. 44, no. 1, Jan. 1984.

[9] R. P. Vasquez, M. H. Hecht, F. J. Grunthaner, and M. L. Naiman, "X-Ray photoelectron spectroscopy study of the chemical structure of thermally nitrided SiO_2," *Appl. Phys. Lett.*, vol. 44, no. 10, pp. 969–971, May 1984.

[10] D. Briggs and M. P. Seah, *Practical Surface Analysis.* New York: Wiley, 1983.

[11] F. L. McCrackin, E. Passaglia, R. R. Stromberg, and H. L. Steinberg, J. Res. Natn. Bureau Standards 67A, p. 363, 1963.

[12] F. L. McCrackin," Analyses and correction of instrumental error in ellipsometry," *J. Opt. Soc. Amer.*, vol. 60, pp. 57–63, 1970.

[13] E. Schmidt, "Precision of ellipsometric measurement," *J. Opt. Soc. Amer.*, vol. 60, pp. 490–494, 1970.

[14] J. R. Zeidler, R. B. Kohles, and N. M. Bashara, "Sensitivity of the ellipsometric parameters to angle-of-incidence variations," *Appl. Opt.*, vol. 13, pp. 1591–1594, 1974.

[15] G. H. Bu-Abbud and N. M. Bashara, "Optimizing null ellipsometry for oxidized silicon," *Appl. Opt.*, vol. 20, pp. 2815–2818, 1981.

[16] K. Riedling, "Error effects in the ellipsometric investigation of thin films," *Thin Solid Films*, vol. 75, pp. 355–369, 1981.

[17] D. Chandler-Horowitz, "Ellipsometric accuracy and the principal angle of incidence," *Integrated Circuit Meytology*, SPIE, vol. 342, p. 121, 1982.

[18] S. S. Samuel, "Ellipsometric analysis for an absorbing surface film on an absorbing substrate with or without an intermediate surface layer," *Surface Sci.*, vol. 56, pp. 97–108, 1976.

[19] J. C. Charmet and P. G. de Gennes, "Ellipsometric formulas for an inhomogeneous layer with arbitrary refractive index profile," *J. Opt. Soc. Amer.*, vol. 73, pp. 1777–1784, 1983.

[20] J. H. Ho, C. L. Lee, C. W. Jen, and T. F. Lei, "Ellipsometry measurement on SiO_2 films for thinkness under 200 Å," *Solid-State Electron.*, vol. 30, pp. 973–981, 1987.

[21] J. H. Ho, C. L. Lee, and T. F. Lei, "Error reduction in the ellipsometric measurement on thin transparent film," *Solid-State Electron.*, vol. 31, pp. 1321–1326, 1988.

[22] J. H. Ho, "A study of the ellipsometry measurement on thin films," Ph.D. dissertation, Institute of Electronics, National Chiao Tung University, pp. 161–165, 1988.

[23] B. Z. Chang, T. F. Lei, C. L. Lee, and J. H. Ho, *Electron Devices and Materials Symp.*, R.O.C., pp. 134–137, 1987.